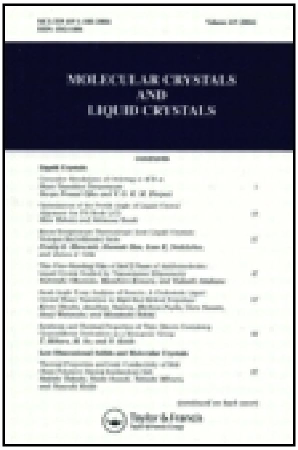

Molecular Crystals and Liquid Crystals Science and Technology. Section A. Molecular Crystals and Liquid Crystals
Publication details, including instructions for authors and subscription information:
http://www.tandfonline.com/loi/gmcl19

Temperature Dependence of the Pretilt Angle for Liquid Crystals: A Comparison Between Theories and Experiments

B. O. Myrvold [a] [b] , M. Isogai [a] & K. Kondo [a]
[a] Hitachi Research Laboratories, 1-10h-mika-cho 7-chome, Hitachi-shi, Ibaraki-ken, 319-12, Japan
[b] Department of Chemistry, University of Oslo, Blindern, P.O. Box 1033, N-0315, Oslo, Norway
Version of record first published: 23 Sep 2006.

To cite this article: B. O. Myrvold , M. Isogai & K. Kondo (1995): Temperature Dependence of the Pretilt Angle for Liquid Crystals: A Comparison Between Theories and Experiments, Molecular Crystals and Liquid Crystals Science and Technology. Section A. Molecular Crystals and Liquid Crystals, 259:1, 115-132

To link to this article: http://dx.doi.org/10.1080/10587259508038677

Mol. Cryst. Liq. Cryst., 1995, Vol. 259, pp. 115–132
Reprints available directly from the publisher
Photocopying permitted by license only

Temperature Dependence of the Pretilt Angle for Liquid Crystals: A Comparison Between Theories and Experiments

B. O. MYRVOLD*, M. ISOGAI and K. KONDO
Hitachi Research Laboratories, 1–1 Oh-mika-cho 7-chome, Hitachi-shi, Ibaraki-ken, 319-12 Japan

(Received May 9, 1994; in final form July 21, 1994)

Data for the temperature dependence of the pretilt angles for nematic liquid crystal mixtures on a polyimide surface are compared with different theories. It is found that our recently proposed population distribution model can explain all the observations well, when we assume a Boltzmann distribution between the different states. The only exception is one sample with azoxybenzenes, which undergo chemical changes.

Keywords: pretilt angle, temperature dependence, polulation distribution

1. BACKGROUND

The surface alignment of liquid crystals is a critical factor during the manufacture of LCDs. Improvements in this process are needed for improving the performance of the displays, as well as production yields.

There are several classes of theories for the surface alignment, elastic forces,[1] tilted easy axis,[2–4] or population distribution.[5–8] The different theories predict different temperature dependencies for the pretilt angles. The early work[1–4] was mostly compared with data for nematic liquid crystals aligned on silicon oxide surfaces, where elastic forces are thought to play the most important role. On polymer surfaces the situation is more complicated and several forces seem to be involved.

Changes in the pretilt angle of more than 10% with temperature cannot be explained by only geometrical structures.[2] Mada[2] developed a model based on the existence of two different easy axes at the surface, the pretilt would then be a balance between the two different forces and could be expressed as

$$\alpha/S = [kx^2 - 2x + 1]/[1 - kx]^2 \tag{1}$$

with $k = (k_{11} - k_{33})/k_{11}$ and $x = \sin^2 \beta$ where α is a fitting parameter, S is the order parameter of the nematic phase, $k_{11}$is the twist elastic constant, k_{33} the splay elastic constant, and β the pretilt.

---

* Present Address: Department of Chemistry, University of Oslo, P.O. Box 1033 Blindern N-0315 Oslo, Norway

It has been pointed out that α is not easily understood in physical terms,[4] also that the S dependent van der Waals interaction and S^2-dependent surface deformation are combined.[4]

Van Sprang and Aartsen[4] developed another model along the lines of Mada.[2,3] Two preferred directions were introduced, one with respect to the van der Waals interaction and one with respect to the elastic interaction. The total surface energy of the system is then given by

$$F_{tot} = -(1/2)\,c_k(nd_k)^2 - (1/2)\,c_{vdw}(n\,d_{vdw})^2 \tag{2}$$

here d_k is the preferred orientation with respect to elastic forces and d_{vdw} with respect to van der Waals interaction. c_k and c_{vdw} are the strengths of the two forces and vary as S^2 and S, respectively. d_k and d_{vdw} are independent of the liquid crystals used. Minimizing the free energy gives us

$$\cot[2(\beta + \theta_{vdw})] = \cot[2(\theta_{vdw} + \theta_k)] + (c/S)\sin[2(\theta_{vdw} + \theta_k)]^{-1} \tag{3}$$

The angles involved are shown in Figure 1, θ_k and θ_{vdw} are the preferred directions with respect to the elastic and van der Waals interactions respectively. $c = c_{vdw}/c_k$.

Recently a population distribution model has been proposed.[5,6] Sugiyama and co-workers[7] have elaborated on this model under the assumption that the population distribution is due to a mechanical deformation of the surface. They give the following equation:

$$W = (\tfrac{1}{4})[1 - \exp\{-\alpha d\}]\int_0^{a+b+c} \{[k_{22}/\alpha]\,[\partial\theta_1/\partial x]^2 + K\alpha(\theta_1 - \beta)^2\}\,\mathrm{d}x \tag{4}$$

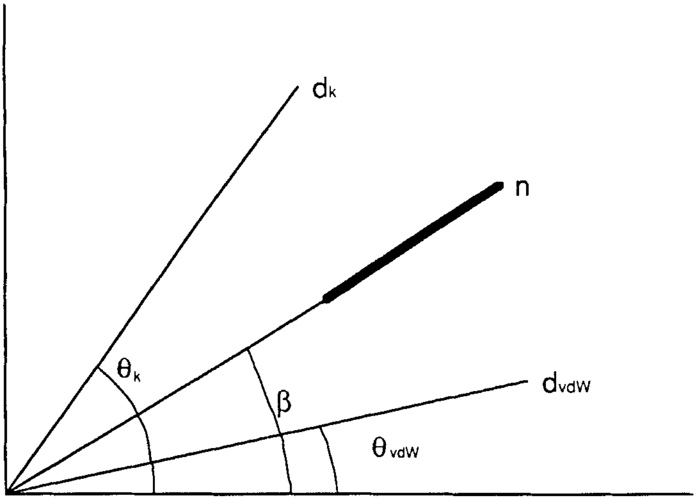

FIGURE 1 The relevant angles in the model of refs. 2–4. d_k and d_{vdw} are the preferred directions with respect to the elastic and van der Waals forces. n is the orientation of the director, which in this model is assumed to be uniform through the structure. β is the pretilt angle, the angle between n and the rubbing direction x.

The pretilt (β) is obtained by minimizing the energy W. θ_1 is the angle of molecules at the surface, α is a correlation length. K is $k_{11} = k_{33}$ and varies as S^2. a, b and c are fitting parameters describing the surface geometries. Figure 2 explain their meaning. As α varies with temperature and must be optimized for each temperature this model contains more adjustable variables than measured points. The authors place some additional constraints on some of the variables from consideration of the rubbing process. However, as long as there are more variables than observed quantities it is of course always possible to obtain perfect fit with any data set. We did thus not perform the calculations for this model.

We[8] have proposed that the population distribution follows a Boltzman distribution, like any other thermo-dynamical equilibrium, and looked at the surface pretilt as caused by the change in distribution between the number of mesogens parallel to the rubbing direction $(1 + a_1)$ and anti-parallel to it $(1 - a_1)$ where this distribution follows the Boltzmanns law. $(1 - a_1)/(1 + a_1) = \exp(-\Delta G/kT)$. Using some standard simplifications we could give the following equation:

$$\beta_{obs} = [\beta_0 - \alpha][c_0 - c_0 \exp(-\Delta G/kT)] \tag{5}$$

where β_{obs} is the observed bulk pretilt, β_0 the angle between the optical axis of the molecules in the first monolayer and the surface, α the angle between the optical and mechanical axis of the mesogens. c_0 is the concentration of molecules in the first mono layer pointing along the rubbing direction, and $c_\pi = c_0 \exp(-\Delta G/kT)$ the number of molecules antiparallel to the rubbing direction. ΔG is the energy difference between the molecules pointing parallel to the rubbing direction and anti-parallel. T is the (absolute) temperature and k Boltzmans constant.

This fitted the data then available well,[8] but can not describe the situation completely.

The maximum relative change in the pretilt due to the change in the population distribution occurs for low energy differences. In the limit of $\Delta G = 0$ the change in the pretilt is given by $\beta_H/\beta_L = T_L/T_H$, where β and T are the observed pretilt and temperature, and the subscripts H and L refer to the high and low temperature. As the energy difference increases the changes in the pretilt decreases. In Figure 3 we have plotted the expected changes in pretilt between $-30°C$ and $+90°C$ (squares), or between 0°C and + 60°C (circles) as a function of the free energy difference between the two states. Even for $\Delta G = 0$ the pretilt changes by less than 20% between 0 and 60°C. As we will see shortly this is less than what we observe experimentally.

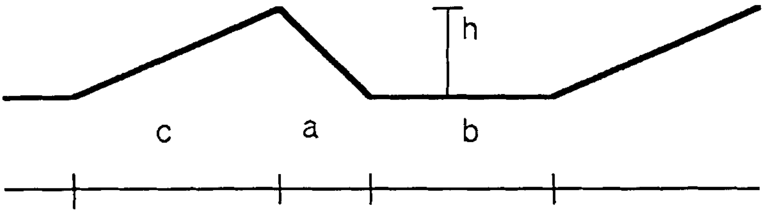

FIGURE 2 The model of the surface employed by Ref. 7.

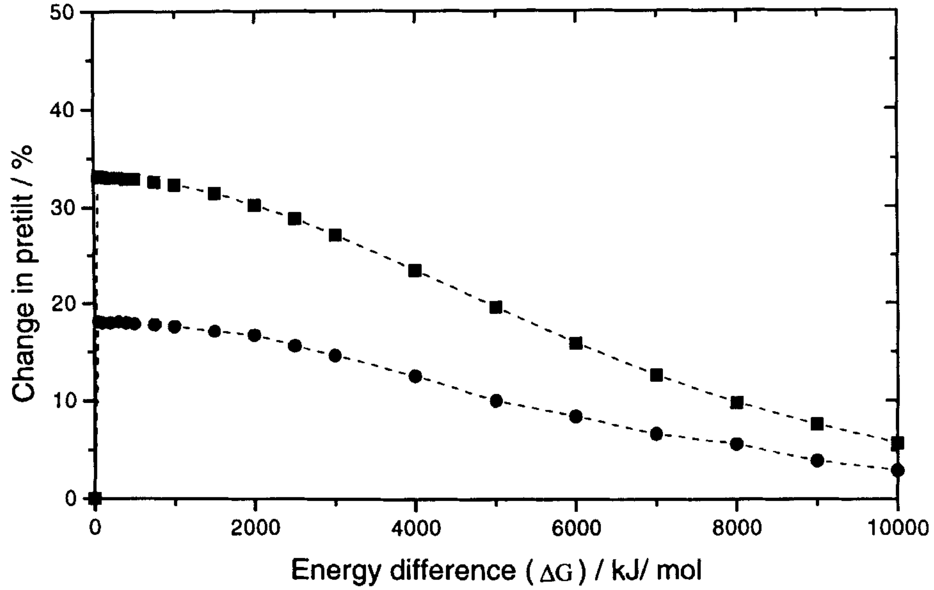

FIGURE 3 Calculated changes in the pretilt between 0 and 60°C (circles) and between – 30 and 90°C (squares) as a function of the free energy difference for the reorientation at the surface.

2. THEORY

Both in the bulk of the nematic liquid crystal and at the surface there is an equilibrium between mesogens as dimers and monomers. This equilibrium is pushed towards the monomers at the surface giving rise to a SHG signal.[9] The strength of the SHG signal and thus presumably also the position of this equilibrium depends on the surface. There are several equilibria, the monomer/dimer equilibrium both at the surface and in the bulk, the adsorption/desorption of monomers and dimers, as well as the parallel and anti-parallel orientation of the monomers. The pretilt in our population distribution model is given by

$$\beta_{obs} = a_1(\beta_0 - \alpha), \tag{6}$$

for thick cells. As we have pointed out before[10] for dimers the in-plane order will be 0, as one of the mesogens in the pair point along the rubbing direction and the other against the rubbing direction. Thus the net contribution to the pretilt from the dimeric pair is zero. Among the monomers more will point along the rubbing direction than opposed to it,[5,6] and the monomers will thus give a contribution to the pretilt. We can write the pretilt as

$$\beta_{obs} = c_{monomer}\, a_1(\beta_0 - \alpha) + c_{dimer}\, O \tag{7}$$

Where $c_{monomer} + c_{dimer} = 1$. For the monomer-dimer equilibrium we can write:

$$(1 - c_{monomer}/2)/c^2_{monomer} = K = \exp - (\Delta G/kT) \tag{8}$$

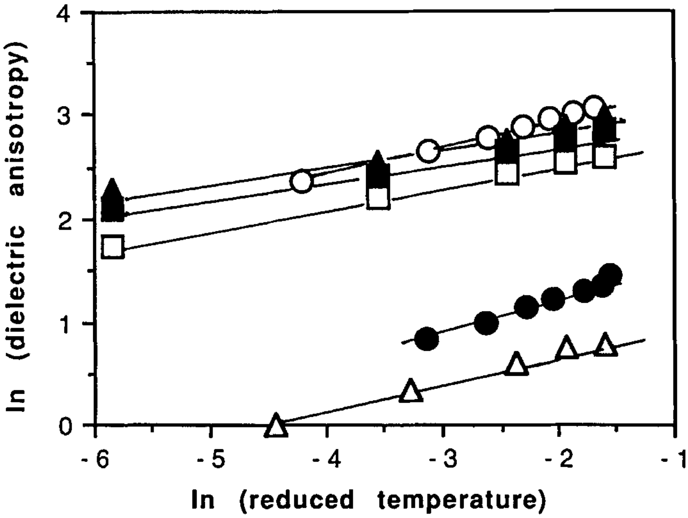

FIGURE 4 A log–log plot of the dielectric anisotropy vs. the reduced temperature for the six liquid crystal used in this study. Top to bottom TN-200, TN-101, E8, ZLI-1132, NP5, HN43.

If the monomer concentration is low we can simplify this as

$$c_{monomer} = \exp(\Delta G/2kT) \tag{9}$$

Combining Equations 8,9 and 6, and taking the logarithm we obtain the following equation:

$$\ln(\beta_{obs}) = \Delta G/2kT + \ln a_1 + \ln(\beta_0 - \alpha) = \Delta G/2kT + Const. \tag{10}$$

As we saw in Figure 3 a_1 will show some temperature dependence, but this is rather small and we have neglected it.

From Equation 10 we can easily make a few predictions. For liquid crystals that do not form dimers the dimer-monomer equilibrium is entirely over on the monomer side and there will be no changes in the equilibrium with temperature. This will give only a small temperature dependence of the pretilt. In this case the weak temperature dependence of a_1 will be important. Except for the factor 1/2 Equation 10 is the same we have given earlier, although the physical background is different. We have previously neglected changes in c_0 with temperature. This time we neglect changes in a_1, as they will be small.

3. EXPERIMENTS

The mixtures are all commercially available except HN-43 which was synthesised in this group. The mixtures used cover six different classes of liquid crystals, although TN-200 and NP5 now is of more historical than practical interest. The structures of the different mixtures are shown in Figures 5–10. NP5 and HN43 were doped with 10% 4-cyano-phenyl-4'-butyl-benzoate (equal to R = n-butyl in the TN 101 structure) to give a positive dielectric anisotropy, for reasons that are not relevant to this study.

The polyimide PIQ (from Hitachi Chemicals) was used for all the test cells. The rubbing conditions were the same for all samples. 20 micron thick cells with anti-parallel rubbing directions were used for the measurements. The crystal rotation method as described earlier[11] was used for the determination of the pretilt angles. We estimate the accuracy in the pretilt angles to be better than +/− 0.3°.

It is found that our recently proposed population distribution model can explain all the observations well, except for one sample with azoxybenzenes, which undergo chemical changes.

4. RESULTS AND DISCUSSION

4.1 Determination of the Order Parameter

Equations 1 and 2 require knowledge of the order parameters. The dielectric anisotropy was measured and the order parameter fitted by $\Delta\varepsilon/C = S = [(T_{ni} - T)/T_{ni}]^b$.

In Figure 4 this is shown in the form of a log–log plot which gives us b directly. As can be seen the lines are parallel thus giving the same b. The constant C will be a material parameter depending on the liquid crystal used, but we do not need to know this to determine S.

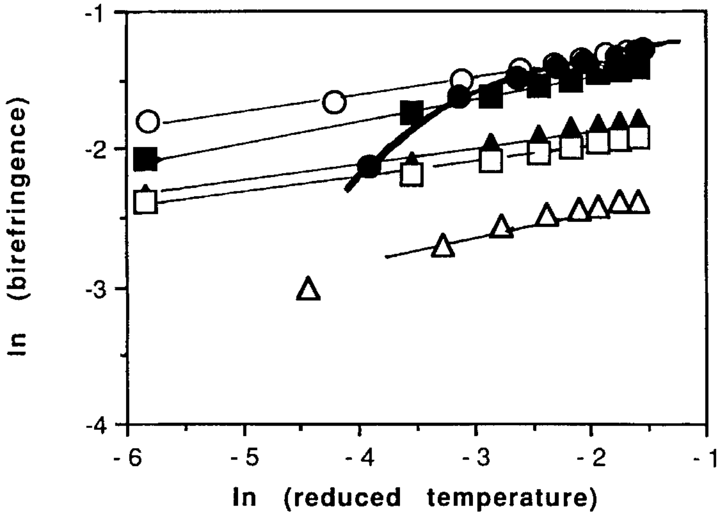

FIGURE 5 A log–log plot of the birefringence vs. the reduced temperature for the six liquid crystals used in this study. Symbols as for Figure 2. Notice how the azoxy mixture NP5 strongly deviates from the expected straight line.

Figure 5 shows a similar plot using the birefringence. We find the same b value for all the liquid crystal, except NP5, from this plot as by using the dielectric anisotropy. We will return to the anomaly of NP5 under 5.9.

4.2 Elastic Constants

For Equation 1 we also need to know the elastic constants. These values are not available. We thus used the simple assumption that $k_{11} = k_{33}$ this give $k = 0$ and simplifies the equation. It does however not influence the results much. Putting $k = -1$ instead of 0 only gave a 0.3% change in the fitting parameter α, at room temperature.

4.3 The Parameters of van Sprang and Aartsen

The two preferred surface direction with respect to van der Waals and elastic interactions are independent of temperature and liquid crystal. We obtained these by fitting the data for E8 for the whole temperature interval investigated. E8 was chosen as this liquid crystal showed the largest variation in the pretilt. From this fit we obtained $\theta_k = 10°$ and $\theta_{vdw} = -3°$.

The constant c is independent of the temperature, but will depend on the liquid crystal used. For E8 c was determined during the fit of the two preferred directions and found to be 0.82.

For the other liquid crystals we used the observed pretilt at 20°C together with $\theta_k = 10°$ and $\theta_{vdw} = -3°$ to obtain the c-values given in Table I.

With θ_k, θ_{vdw} and c known, β as a function of S can be obtained easily from Equation 3. Since we know how S varies with T this gives us the temperature variation of β.

The calculations were all performed with a hand-held calculator (Sharp EL-509D), or the in-built functions in the Cricket Graph program.

4.4 The Cyanobiphenyl Mixture E8

The experimental results for this mixture, together with the theoretical curves are given in Figure 6. We see that one temperature dependent easy axis as assumed by Ref. 2 is

TABLE I

The fitting parameter (c) for the liquid crystal mixtures used in this study.

Liquid crystal	c
E8	0.82
NP5	0.90
RO-TN-200	0.97
RO-TN-101	1.02
ZLI-1132	1.21
HN43	1.26

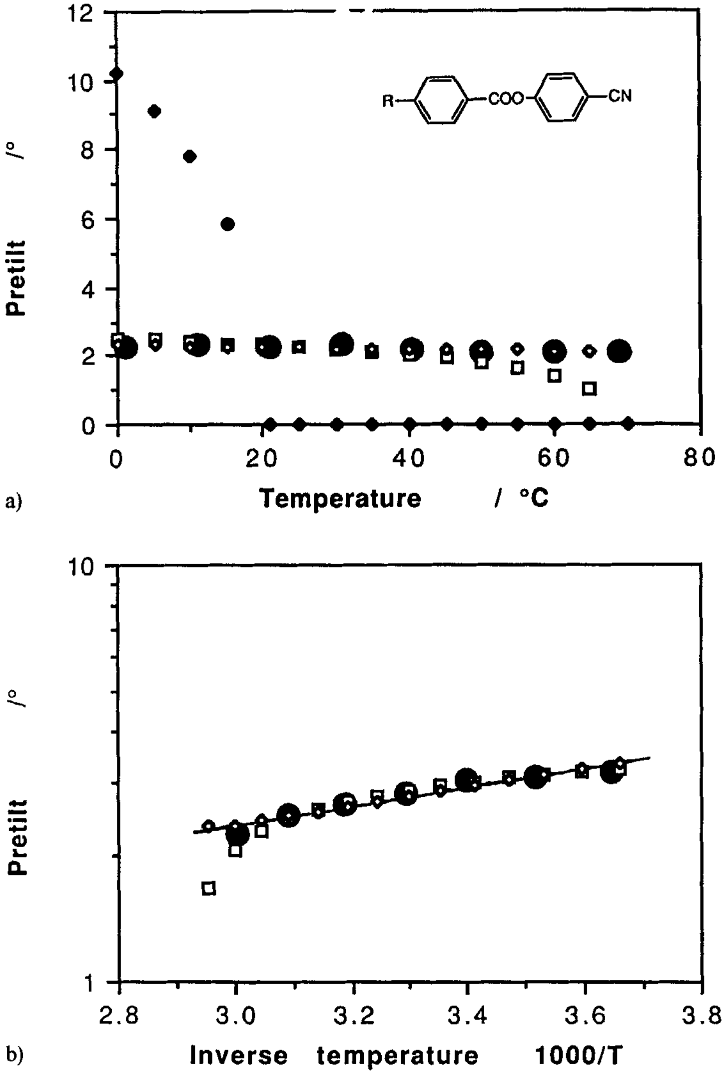

FIGURE 6 The temperature dependence of the pretilt for E8. Filled circles experimental data. Filled diamonds after Equation 1. Open squares after Equation 2. Open diamonds after Equation 5. A) Plot of pretilt vs. temperature. b) Plot of the logarithm of pretilt vs. inverse temperature, to show the near linearity. Only the two best theoretical fits are shown in this plot.

not able to reproduce the data. The theory of van Sprang and Aartsen[4] with two temperature independent easy axes and the pretilt resulting from the order parameter dependent balance between the two gives excellent fit to the data. But it should be remembered that this was also the data set that was used for extracting the easy axis orientations.

Our model based on the population distribution does only deviate from the two easy axes model close to the phase transition. For E8 the fit by our model and the model with two easy axes are the same, In Figure 6B we have transformed the plot into a form which allows us to extract ΔG, the energy difference for the dimer-monomer equilibrium at the surface directly. The value we find is 8.8 kJ/mol.

4.5 The Cyanophenyl-Cyclohexane Mixture ZLI-1132

The comparison between theory and experiment is shown in Figure 7. As for E8, and also the rest of these mixtures the temperature dependent easy axis is not able to

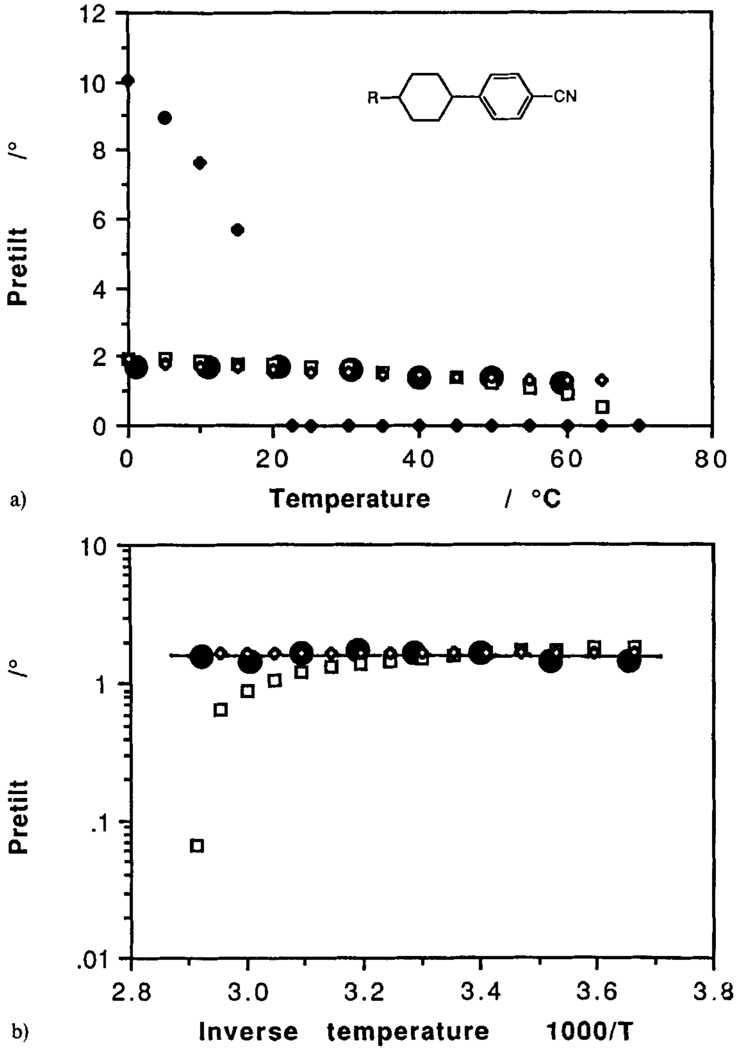

FIGURE 7 The temperature dependence of the pretilt for ZLI-1132. Filled circles experimental data. Filled diamonds after Equation 1. Open squares after Equation 2. Open diamonds after Equation 5 A) Plot of pretilt vs. temperature. b) Plot of the logarithm of pretilt vs. inverse temperature, to show the near linearity. Only the two best theoretical fits are shown in this plot.

describe the experiments well. Although we will show the data, the fit will not be commented upon in the rest of the cases.

The model with two fixed easy axes over estimates the temperature dependence for this liquid crystal slightly (this is easiest to see in Figure 7B). Within the experimental error it is not possible to decide between one model or the other.

The population distribution model gives an excellent fit to the data. As we have shown before the PCH liquid crystals are slightly more bent than the CB type. This means that α in Equation 9 is larger. Thus it is also expected that ZLI-1132 shows a somewhat lower pretilt than E8. The energy difference between the monomer and the dimer on the surface for ZLI-1132 is 9.0 kJ/mol. This is the same value as for E8. Second harmonic generation (SHG) measurements[9] have shown that the cyano group points into the surface. Thus it will be the same cyano-phenyl group interacting with the surface in both of these cases, it is thus not surprising that the energy difference should be similar.

4.6 The Cyano-ester Mixture TN-101

The data and calculations are shown in Figure 8. The results are similar to the one shown before, although the model with two easy axis give somewhat poorer fit for this liquid crystal than for the previous two.

The population distribution model gives excellent fit, but the energy difference is only 3.2 kJ/mol for this mixture. Also in this case we have the same cyano-phenyl group presumably interacting with the surface as for E8 and ZLI-1132, it is thus surprising that the energy difference is only 1/3. These molecules do, however, also contain other dipoles in the ester group, and the interactions might be more complicated in this case.

4.7 The Schiff Base Mixture TN-200

The theoretical and experimental values are shown in Figure 9. Again we find that the population distribution model gives a slightly better fit than the model with two easy axes. The energy difference between the two states is found to be a little lower than for TN-101, 2.0 kJ/mol in this case.

4.8 The Dialkyl-ester Mixture HN43

The experimental data for this mixture are scattered slightly more than for the other mixtures (Figure 10). A best linear fit to the data will actually show a tiny increase in the pretilt angle with temperature. The model with two easy axes is not very successful in describing these data. For this mixture of dialkyl compounds we do not expect any dimer formation, and thus there are no changes in the population at the surface either.

4.9 The Azoxy Mixture NP5

This mixture gave an unexpected behaviour, with a clear and fairly large increase in the pretilt with temperature (Figure 11). As can be seen none of the theories can explain

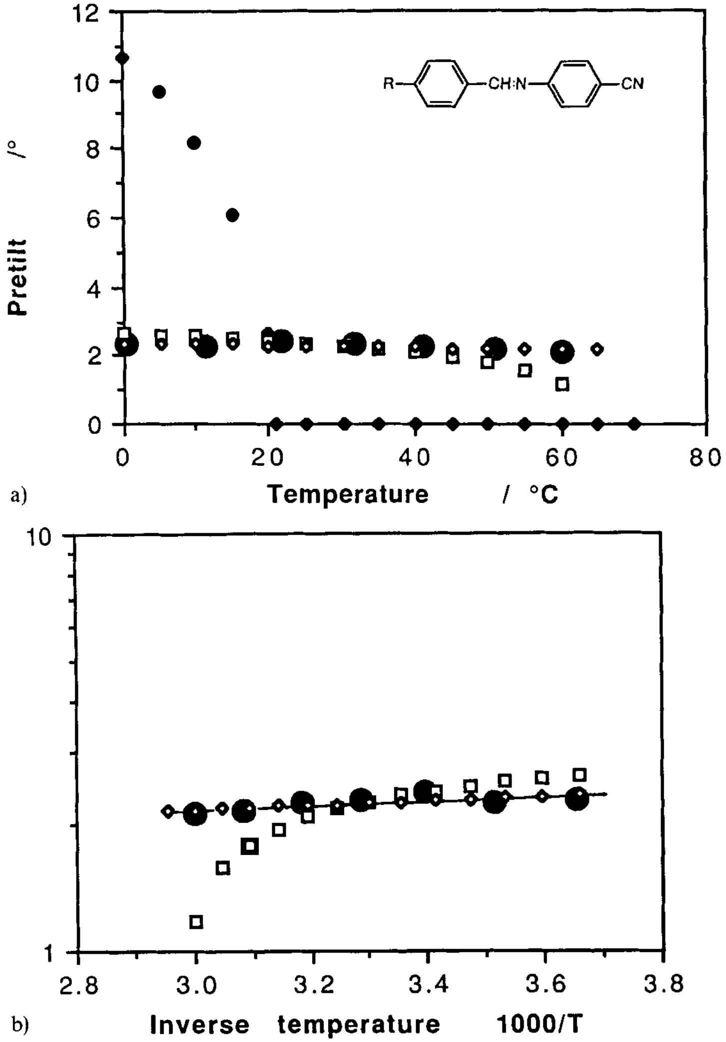

FIGURE 8 The temperature dependence of the pretilt for TN-101. Filled circles experimental data. Filled diamonds after Equation 1. Open squares after Equation 2. Open diamonds after Equation 5. A) Plot of pretilt vs. b) Plot of the logarithm of pretilt vs. inverse temperature temperature, to show the near linearity. Only the two best theoretical fits are shown in this plot.

this. We have not even tried to calculate the pretilt from the population distribution model.

As Figure 11B shows we still obtain a nearly linear plot indicating that the system follows the Boltzman distribution in some way. However, the energy difference of − 8.0 kJ/mol indicates that the lowest energy state is least populated. This is clearly an impossible result.

The structure of NP5 shown in Figure 11A is really a short hand notation. What we have is a mixture of the two position isomers shown in Figure 12. If we assume an

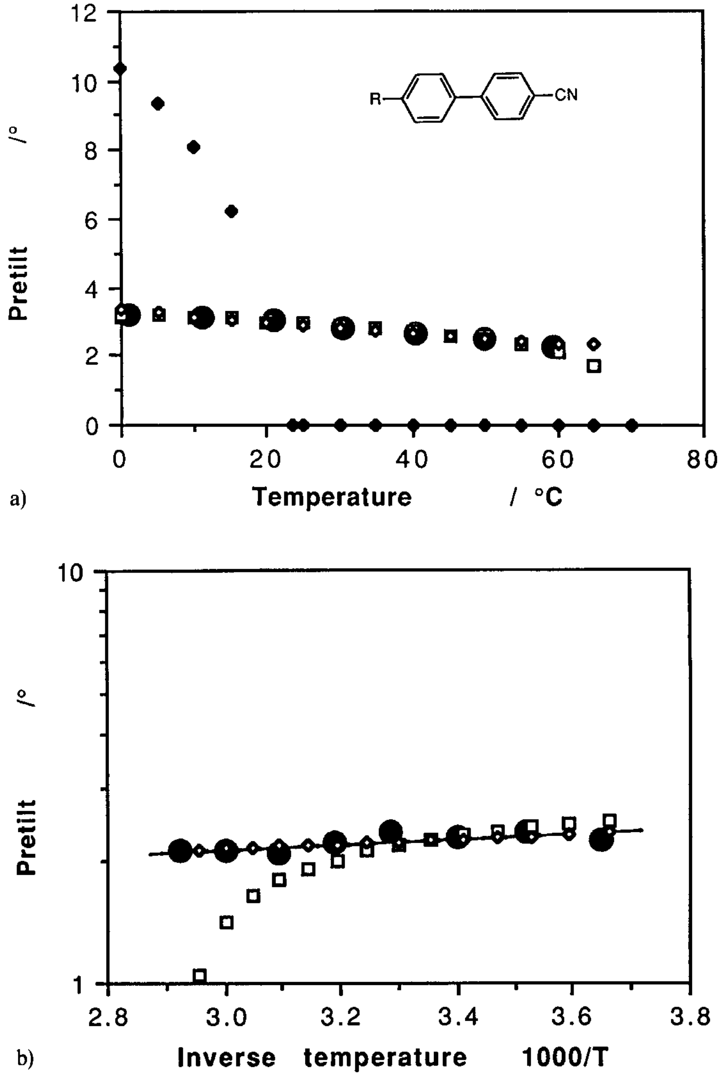

FIGURE 9 The temperature dependence of the pretilt for TN-200. Filled circles experimental data. Filled diamonds after Equation 1. Open squares after Equation 2. Open diamonds after Equation 5. A) Plot of pretilt vs. temperature. b) Plot of the logarithm of pretilt vs. inverse temperatue, to show the near linearity. Only the two best theoretical fits are shown in this plot.

equilibrium between the two forms the composition of the mixture is no longer constant. In other words the term $\beta_0 - \alpha$ in Equation 10 is no longer independent of temperature. As we found for HN 43 the pretilt hardly changes over the temperature interval for the dialkyl compound. We except the same for NP5 as there are no dimer monomer equilibrium here, either. But for NP5 we have the added complication that the shape, and possibly the orientation, of the molecules changes.

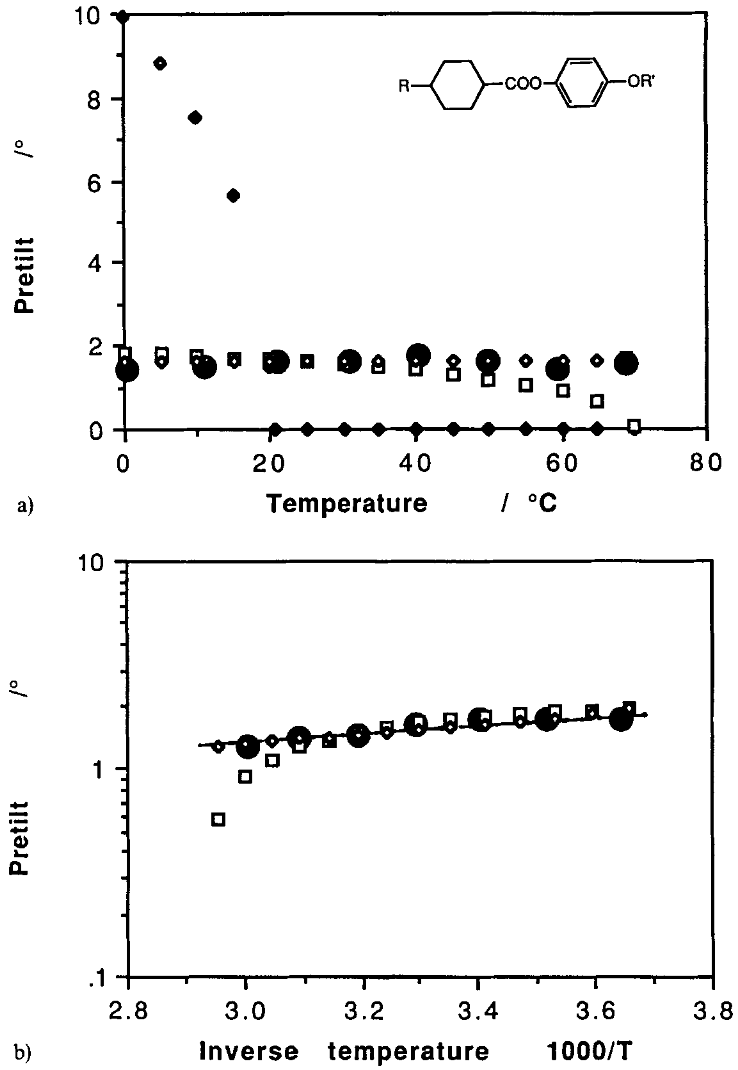

FIGURE 10 The temperature dependence of the pretilt for HN43. Filled circles experimental data. Filled diamonds after Equation 1. Open squares after Equation 2. Open diamonds after Equation 5. A) Plot of pretilt vs. temperature. b) Plot of the logarithm of pretilt vs. inverse temperature, to show the near linearity. Only the two best theoretical fits are shown in this plot.

If there is an equilibrium between two different isomers this will, like any other chemical equilibrium, follow the Boltzman distribution. As we saw in Figure 11B this system does appear to follow a Boltzman distribution.

The data for the birefringence of NP5, shown in Figure 5, shows that for this mixture the birefringence is not a simple function of the temperature, or order parameter. Although we can not rule out other possibilities the anomalous behaviour do support

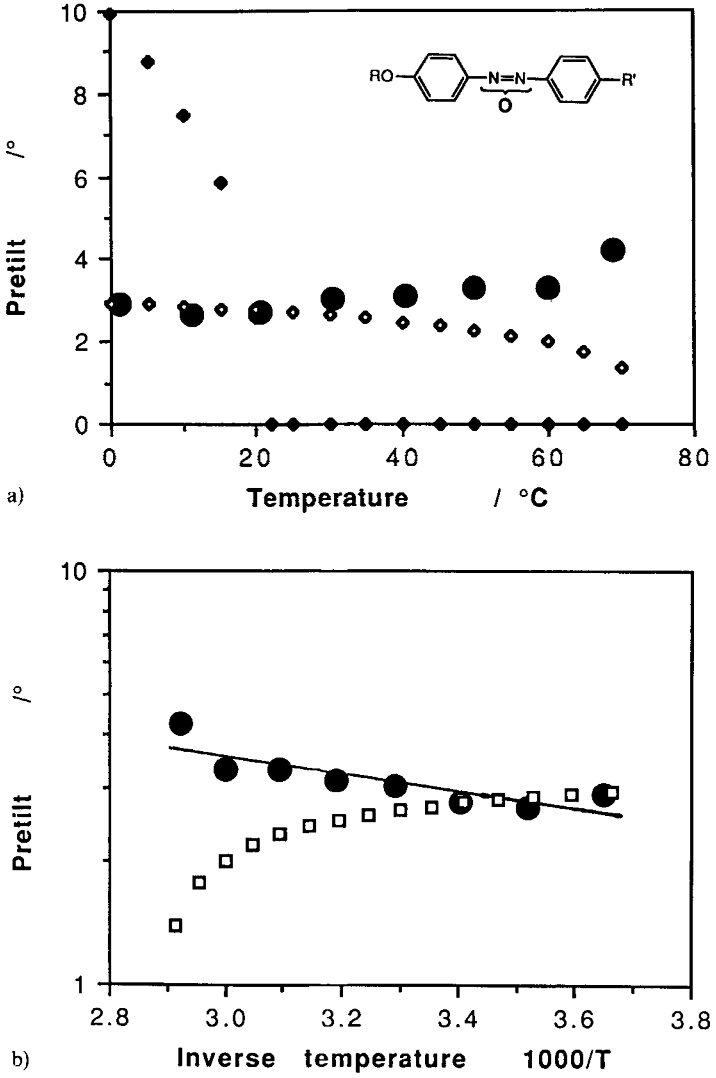

FIGURE 11 The temperature dependence of the pretilt for NP5. Filled circles experimental data. Filled diamonds after Equation 1. Open squares after Equation 2. Open diamonds after Equation 5. A) Plot of pretilt vs. temperature. b) Plot of the logarithm of pretilt vs. inverse temperature, to show the near linearity. Only the two best theoretical fits are shown in this plot.

the hypothesis that chemical changes are taking place. Due to the different electron withdrawing and donating capabilities of the alkoxy-and alkyl-chains the electronic properties of 12A and 12B will be different, giving rise to difference in the birefringence. For the dielectric anisotropy, which is measured at low frequency, permanent dipoles are also contributing. The strength of these are less influenced by the changes between 12A and 12B, thus the similar deviation from ideal behaviour is not observed in Figure 4.

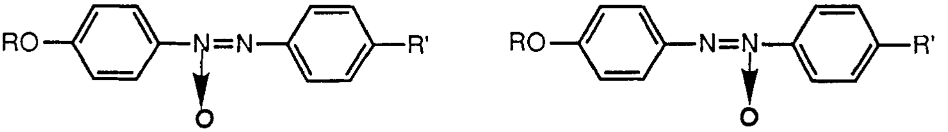

12A **12B**

FIGURE 12 The two isomeric structures of the azoxy compounds NP5.

If chemical changes takes place we can of course no longer assume that the elastic expressions, *k* of Mada[2,3] or *c* of van Sprang and Aartsen[4] are independent of temperature, either.

4.10 Previous Experiments

The results of our investigation shows that the population distribution model best describes the data for the temperature dependence of the pretilt angle. We now want to show that this model also can explain older results from the literature.

There are only few studies of the temperature dependent pretilt on polymer surfaces. The first and most interesting is by the Merck group.[12] This investigation covers several liquid crystals over a very broad temperature range. The polyimide used is SE-4110. We have replotted their data in Figure 13. For four of the mixture we find nearly the same energy difference of 3.8–4.8 kJ/mol. For the experimental mixture

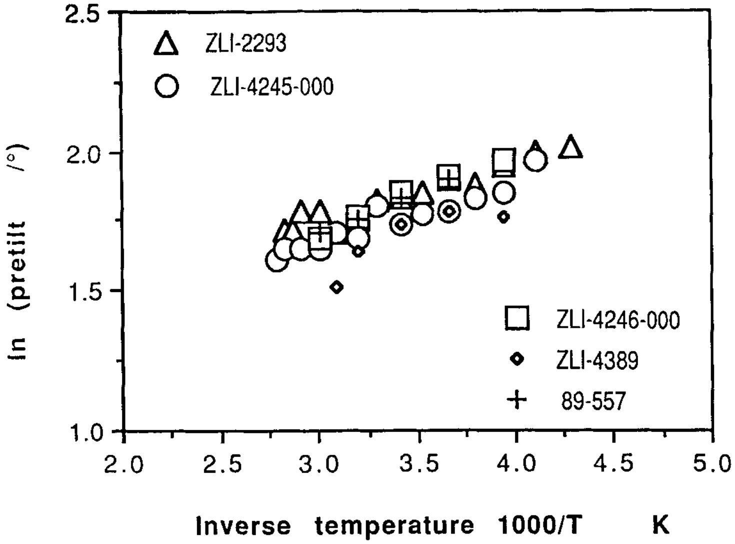

FIGURE 13 The data of Ref. 12 for the temperature dependence of the pretilt angle plotted as logarithm of the pretilt vs. inverse temperature. As can be seen for all five mixtures the data fall on a straight over a wide temperature range.

89-557 the energy difference is much higher (13.8 kJ/mol). As can be seen from Figure 13 these data are all very close to the straight lines and are thus in excellent agreement with our population distribution model.

The results of another investigation from the same group[13] is shown in Figure 14. Here the two superfluorinated mixtures MLC-2016 and MLC-2019 are aligned by the two polyimides called PI-1 and PI-3. Again we see that there is a good linear relationship between the logarithm of the pretilt angle and the inverse temperature over a wide temperature range (from −20°C to +60°C). We find energy differences of 17.2 kJ/mol (MLC-2019) and 9.8 kJ/mol (MLC-2016) on PI-1. On the polyimide PI-3 the differences are higher for both nematic mixtures, 19.6 kJ/mol for MLC-2019 and 13.4 kJ/mol for MLC-2016.

A recent work[7] has looked at the pretilt of 5CB at two different polyimide surfaces. Surfaces *A* and *B* have alkyl branches, but are rubbed differently, while *C* is a simple unbranched polyimide. We find that the population distribution model describes the pretilt well also for these three systems (Figure 15). For the three systems we obtain $\Delta G = 10.1$ kJ/mol for surface *A*, 7.9 kJ/mol for *B* and 5.6 kJ/mol for *C*.

The authors use a population distribution model to explain their data. In their model the surface is physically deformed, and there is a distribution of molecules tilting in different directions at the surface (as shown in Figure 2). The observed pretilt is the average over this surface distribution. This model is similar to that proposed by Nakamura.[14] The bulk pretilt calculated by Ref. 7 is in the opposite direction of that calculated by Ref. 14, relative to the asymmetry of the surface deformations.

We will suggest a reinterpretation of the authors fitting parameter. We refer to Figure 2 for a definition of the different quantities. We combine their different surface

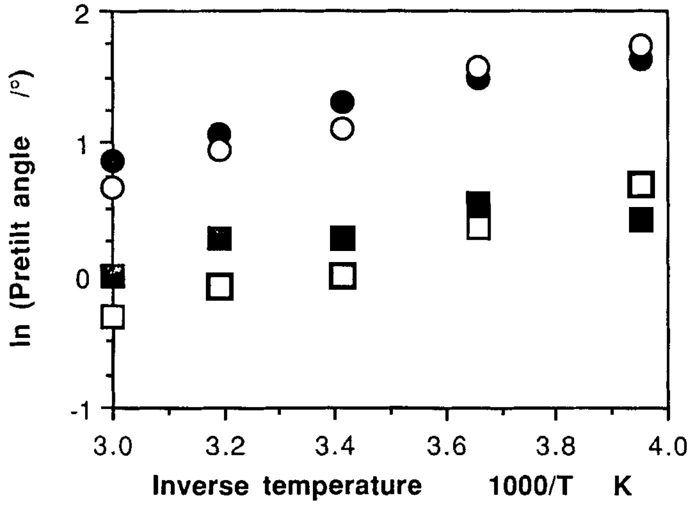

FIGURE 14 The data of Ref. 13 for the temperature dependence of the pretilt angle plotted as logarithm of the pretilt vs. inverse temperature. For both mixtures used on both surfaces the data fall on a straight over a wide temperature range. Circles PI-3, squares PI-1, filled symbols MLC-2016, open symbols MLC-2019.

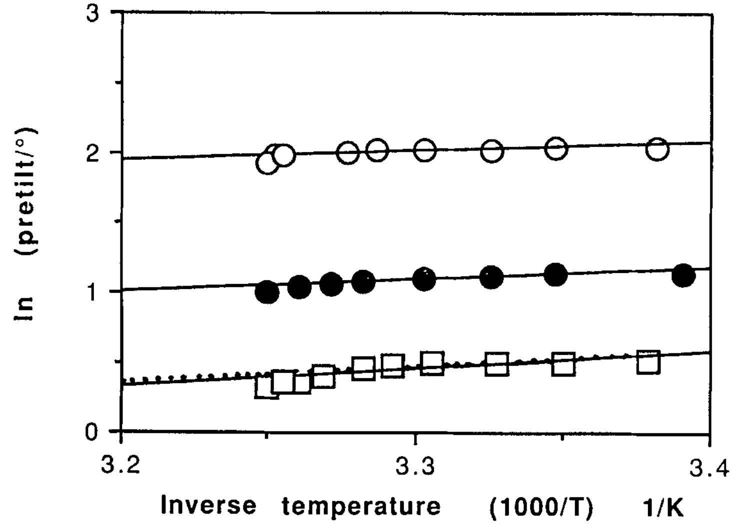

FIGURE 15 The data of Ref. 7 for the temperature dependence of the pretilt angle plotted as logarithm of the pretilt vs. inverse temperature. For all three polyimides the data fall on a straight, with a possible slight deviation close to the clearing point. The dotted line for surface C is calculated from our reinterpretation of the fitting parameters of Ref. 7. See 4.10 for details of the reinterpretation.

inclinations to give the surface distribution.

$$b/(a+c)^2 = K = \exp(-\Delta G/kT) \tag{11}$$

in other words c corresponds to an area with perfect parallel order, a to an area with perfect anti-parallel order and b to an area with dimers. We can also find the asymmetry for the monomers as:

$$a_1 = (a-c)/(a+c) \tag{12}$$

We thus simplify their distribution over three different states to one over two different states. From the values given by Ref. 7 we obtain $a_1 = (26-4)/(4+26) = 0.733$ and $\Delta G = RT \ln K = 9.4\,\mathrm{kJ/mol}$, which is in excellent agreement with the 10.1 kJ/mol obtained from the best fit to Equation 10.

$\beta_0 - \alpha$ can be expressed by a,b,c and h. We notice that our model requires three independent parameters ΔG, c_0 and $\beta_0 - \alpha$ when the liquid crystal and surface is kept constant. The model of Sugiyama *et al.*[7] on the other hand requires seven (a,b,c and h related to the shape of the surface A_θ the surface energy, the elastic constant K, and α a temperature dependent correlation length).

There is one work showing a temperature dependence of the pretilt for E8 on PVA.[15] However, the differences in the pretilts are small, and the authors fails to take account the temperature dependencies of the refractive indexes in their measurements.

5. CONCLUSIONS

At the surfaces there are two temperature dependent equilibria. One is the dimer-monomer equilibrium, and the other is the population difference between monomers pointing parallel and anti-parallel to the rubbing direction. We can neglect the second equilibrium and still obtain an excellent agreement between the theoretical and experimental temperature dependence of the bulk pretilt from the population distribution model and experimental data.

References

1. D. W. Berreman, *Phys. Rev. Lett.*, **28**, 1683 (1972).
2. H. Mada, *Mol. Cryst. Liq. Cryst.*, **51**, 43 (1979).
3. H. Mada, *Mol. Cryst. Liq. Cryst.*, **53**, 127 (1979).
4. H. A. van Sprang and R. G. Aartsen, *J. Appl. Phys.*, **56**, 251 (1984).
5. M. Barmentlo, R. W. J. Hollering and N. A. J. M. van Aerle, *Phys. Rev.*, *A* **46**, R4490 (1992).
6. M. Barmentlo, R. W. J. Hollering and N. A. J. M. van Aerle, *Liq. Cryst.*, **14**, 475 (1993).
7. T. Sugiyama, S. Kuniyasu and S. Kobayashi, *Mol. Cryst. Liq. Cryst.*, **231**, 199 (1993).
8. B. O. Myrvold, K. Kondo, *Liq. Cryst.*, in the press (LC 3.10/875), (1994).
9. M. B. Feller W. Chen and Y. R. Shen *Phys. Rev.*, *A* **43**, 6778 (1991).
10. B. O. Myrvold, K. Kondo, submitted to *Liq. Cryst.*, (1994).
11. F. Nakano, M. Isogai and M. Sato, *Jpn. J. Appl. Phys.*, **19**, 2013 (1980).
12. G. Weber, H. J. Plach, S. Naemura and B. Scheuble, *Proc. Japan Display* **89** 532 (1989) Kyoto.
13. H. J. Plach, E. Bartmann, E. Poetsch, K. Kobayashi, A. Sawada and B. Rieger, *Proc. 6th Liq. Cryst. Sem.* (Merck) 37 (1992) Tokyo/Osaka.
14. M. Nakamura, *J. Appl. Phys.*, **52**, 4561 (1981).
15. I. A. Khan, J. Iqbal, S. M. Afzal and R. Mahmood, 14 th Int LC. Conf. Pisa (1992).